Targeting Nicotinamide *N*-Methyltransferase and miR-449a in EGFR-TKI-Resistant Non-Small-Cell Lung Cancer Cells

Duc-Hiep Bach,[1] Donghwa Kim,[1] Song Yi Bae,[1] Won Kyung Kim,[1] Ji-Young Hong,[1] Hye-Jung Lee,[1] Nirmal Rajasekaran,[2] Soonbum Kwon,[2] Yanhua Fan,[1] Thi-Thu-Trang Luu,[1] Young Kee Shin,[2] Jeeyeon Lee,[2] and Sang Kook Lee[1]

[1]College of Pharmacy, Natural Products Research Institute, Seoul National University, Seoul, Korea; [2]College of Pharmacy, Research Institute of Pharmaceutical Sciences, Seoul National University, Seoul, Korea

Epidermal growth factor receptor tyrosine kinase inhibitors (EGFR-TKIs) are used clinically as target therapies for lung cancer patients, but the occurrence of acquired drug resistance limits their efficacy. Nicotinamide *N*-methyltransferase (NNMT), a cancer-associated metabolic enzyme, is commonly overexpressed in various human tumors. Emerging evidence also suggests a crucial loss of function of microRNAs (miRNAs) in modulating tumor progression in response to standard therapies. However, their precise roles in regulating the development of drug-resistant tumorigenesis are still poorly understood. Herein, we established EGFR-TKI-resistant non-small-cell lung cancer (NSCLC) models and observed a negative correlation between the expression levels of NNMT and miR-449a in tumor cells. Additionally, knockdown of NNMT suppressed p-Akt and tumorigenesis, while re-expression of miR-449a induced phosphatase and tensin homolog (PTEN), and inhibited tumor growth. Furthermore, yuanhuadine, an antitumor agent, significantly upregulated miR-449a levels while critically suppressing NNMT expression. These findings suggest a novel therapeutic approach for overcoming EGFR-TKI resistance to NSCLC treatment.

INTRODUCTION

Lung cancer remains the leading cause of cancer death worldwide, with two main histological groups: small cell lung cancer (SCLC) and non-small-cell lung cancer (NSCLC), which represents 85% of all lung cancer cases.[1] Despite progress in therapeutic strategies for advanced NSCLC, the curative effects seem to have reached a plateau, and patient prognosis has remained poor. Moreover, studies examining the activation of specific genes in EGFR-TKI-resistant NSCLC cells, and the treatment of those overexpressed genes, have not been thoroughly investigated. Subsequently, novel therapeutic approaches are necessarily required to elucidate the molecular mechanisms in drug-resistant cancer cells.

Accumulating evidence suggests that the deregulation of metabolic enzymes might frequently have pro-tumorigenic effects. Nicotinamide

(NCA) *N*-methyltransferase (NNMT) is a cytosolic enzyme that catalyzes the transfer of the methyl group from *S*-adenosyl methionine (SAM) to NCA, generating *S*-adenosylhomocysteine (SAH) and 1-methylnicotinamide (1-MNA).[2] NNMT is overexpressed in a variety of cancers, including liver, kidney, bladder, and colon, and has been shown to promote the migration, invasion, proliferation, and survival of cancer cells.[3–7] Despite considerable experimental evidence that NNMT induces tumorigenesis and may thus represent a potential anti-cancer target, the actual functions of this enzyme in chemo-resistant tumors have not yet been fully investigated, especially in EGFR-TKI-acquired resistant NSCLC cells.

A large body of evidence suggests the critical function of microRNAs (miRNAs) in epigenetically modulating different phenotypic stages in drug-resistant tumors.[8–10] Our recent study also described the role of miRNAs in the regulation of various aspects of tumor progression associated with drug resistance.[11,12] The small, non-coding molecules known as miRNAs elicit their regulatory effects by binding imperfectly to the 3′ UTR of their target mRNA, leading either to degradation of the mRNA or suppression of its translation into functional protein.[13,14] Moreover, the aberrant expression of miRNAs is highly correlated with cancer development.[11,12]

In general, antitumor agents can suppress cancer cell growth through the regulation of cell signal transduction or proliferation.[15–18] Importantly, we have previously found that natural product-derived compounds, including the antitumor agent yuanhuadine (YD), could enhance the antitumor activity of chemo-therapeutic agents through different mechanisms,[19,20] suggesting that these compounds could exert their pleiotropic effects on cancer treatment by regulating various cell signaling pathways. Herein, we attempted to elucidate the role of NNMT in EGFR-TKI resistance in NSCLC cells and the

dynamic interactions of NNMT with miR-449a in a tumor microenvironment. Further studies also suggested that an antitumor agent YD is able to modulate the NNMT and miRNA-449a expression, and thus overcome the acquired drug resistance. These findings will highlight potential new strategies for the treatment of cancer patients with EGFR-TKI-resistant NSCLC.

RESULTS

The NNMT Expression Profile Is Inversely Correlated to miR-449a Expression in Gef-Resistant NSCLC Tissues and Cell Lines

Previous findings suggest that the higher expression of NNMT in tumor tissues is associated with the lower overall survival rates in cancer patients. Therefore, there is an opposite correlation between the expression level of NNMT in tumor tissues and the duration of survival (http://kmplot.com/analysis/index.php?p=service&start=1). Using a cDNA microarray, we have also previously observed high expression of NNMT in EGFR-TKI-resistant cancer cells compared with their parental cells.[21] These findings suggested that NNMT, one of the most overexpressed genes, might be considered a novel target gene in EGFR-TKI-resistant NSCLC cells. Consequently, we initially determined the expression level of NNMT in parental NSCLC cells, including H292 (EGFR wild-type), H1993 (MET amplification), HCC827 (EGFR mutation and MET amplification), and PC-9 (EGFR mutation), versus their EGFR-TKI-resistant NSCLC cells, including gefitinib (gef)- and erlotinib (erl)-acquired cells. We observed overexpression of NNMT mRNA in gef-resistant cells (H292-Gef, H1993-Gef, and PC9-Gef) compared with their parental cells (Figure 1A). A similar phenomenon was also found in erl-resistant cells (H292-Erl, H1993-Erl, HCC827-Erl, and PC9-Erl) (Figure 1B). To validate whether these findings might be associated with NNMT expression in EGFR-TKI-resistant tumors, we also investigated the expression of NNMT in tumor tissues obtained from our previous *in vivo* studies. Confirmation using H292-Gef and PC9-Gef tumor tissues revealed that the levels of NNMT mRNA were also overexpressed in gef-resistant tissues (Figure 1C). Interestingly, we further observed that H1993 cells, which had the highest established gef and erl resistance at 10 μM drug, showed significant NNMT overexpression at both protein and mRNA levels in EGFR-TKI-resistant NSCLC cells compared with their parental cells. Similarly, NNMT protein expression was upregulated in H292-Gef, H1993-Gef (Figure 1D), H1993-Erl, and HCC827-Erl cells (Figure 1E) and in H292-Gef tumor tissues (Figure 1F). Immunohistochemistry (IHC) analyses also illustrated a higher NNMT level in gef-resistant tumors (H292-Gef, H1993-Gef) than in their parental tumors (Figure 1G). Collectively, these data indicated that the basal levels of NNMT expression in gef- or erl-resistant NSCLC cells were overexpressed compared with their parental NSCLC cells.

Recently, miRNAs have been implicated in a wide range of cellular processes, as well as the critical function of miRNAs in the drug resistance of tumor cells, as recently reviewed by our group.[11,22] Among various miRNAs, we initially analyzed miR-449a, which has recently been described to have an important role in resistance to sunitinib, an oral multi-targeted tyrosine kinase inhibitor

(TKI).[23] In addition, miR-449a is downregulated in NSCLC and suppresses cancer cell migration and invasion.[24] Subsequently, we found that miR-449a was downregulated in gef-resistant NSCLC cells compared with their parental cells *in vitro* (Figure 1H) and *in vivo* in tumor tissues (Figure 1I). Furthermore, we observed that miR-449a was also downregulated in H292-Erl and H1993-Erl (Figure 1J). These findings suggested that the expression of NNMT was upregulated, but miR-449a was downregulated, in EGFR-TKI-resistant NSCLC cells.

NNMT Modulates Gef-Resistant NSCLC Cells by Interacting with miR-449a

The effects of NNMT on proliferation and metastatic potential have been reported in cancer cells.[5,7] To investigate whether abnormal overexpression of NNMT is associated with the survival of gef-resistant NSCLC cells subjected to gef resistance, we transfected NNMT small interfering RNA (siRNA) into human gef-resistant NSCLC cells to knock down intracellular NNMT expression. The efficiency of NNMT siRNA was confirmed prior to its use in H1993-Gef cells, which seemed to have the highest levels of NNMT overexpression among other gef-resistant NSCLC cells in this study (Figures S1A and S1B). Subsequently, the effects of NNMT siRNA on the sensitivity of gef were evaluated in gef-resistant NSCLC cells. We found that knockdown of NNMT by siRNA interference restored gef sensitivity to gef-resistant NSCLC cells (Figure 2A; Table 1). Even though at 48 hr, post-siRNA transfection had seemingly no significant effects on G0/G1 phase or G2/M in cell-cycle analysis (Figure 2B), the treatment of NNMT siRNA effectively suppressed colony formation and enhanced activity with co-treatment of gef in gef-resistant NSCLC cells (Figure 2C; Figure S1C). We further assessed the effects of miR-449a on cancer cell growth to determine whether miR-449a expression could alter gef sensitivity in resistant cells. When gef-resistant NSCLC cells were treated with exogenous miR-449a, the cellular level of miR-449a was significantly enhanced (Figure 2D). miR-449a-treated gef-resistant NSCLC cells were cultured in various concentrations of gef (0.4–50 μM gef). As a result, miR-449a transduction significantly increased the gef sensitivity, with at least a 2-fold change in the inhibitory concentration 50% (IC_{50}) for gef (Figure 2E; Table 2), while knockdown of miR-449a enhanced cell proliferation in H292-Gef cells compared with their control (Figure S1D). These data indicated that the level of miR-449a expression affected the gef sensitivity in cancer cells.

To further investigate the possible pathological relevance of the relationship between miR-449a and NNMT in gef-resistant NSCLC cells, we next assumed that the overexpression of NNMT could alleviate the expression of miR-449a in gef-resistant NSCLC cells. Subsequently, bio-informatics analysis (http://www.targetscan.org/vert_71/) led us to focus on NNMT as a possible predicted target of miR-449a via their potential bindings (Figure 2F). When we knocked down NNMT expression by its siRNA, the expression of miR-449a was upregulated in gef-resistant NSCLC cells (Figure 2G). Collectively, these data suggested that NNMT was critical for the suppression of miR-449a in gef-resistant NSCLC cells.
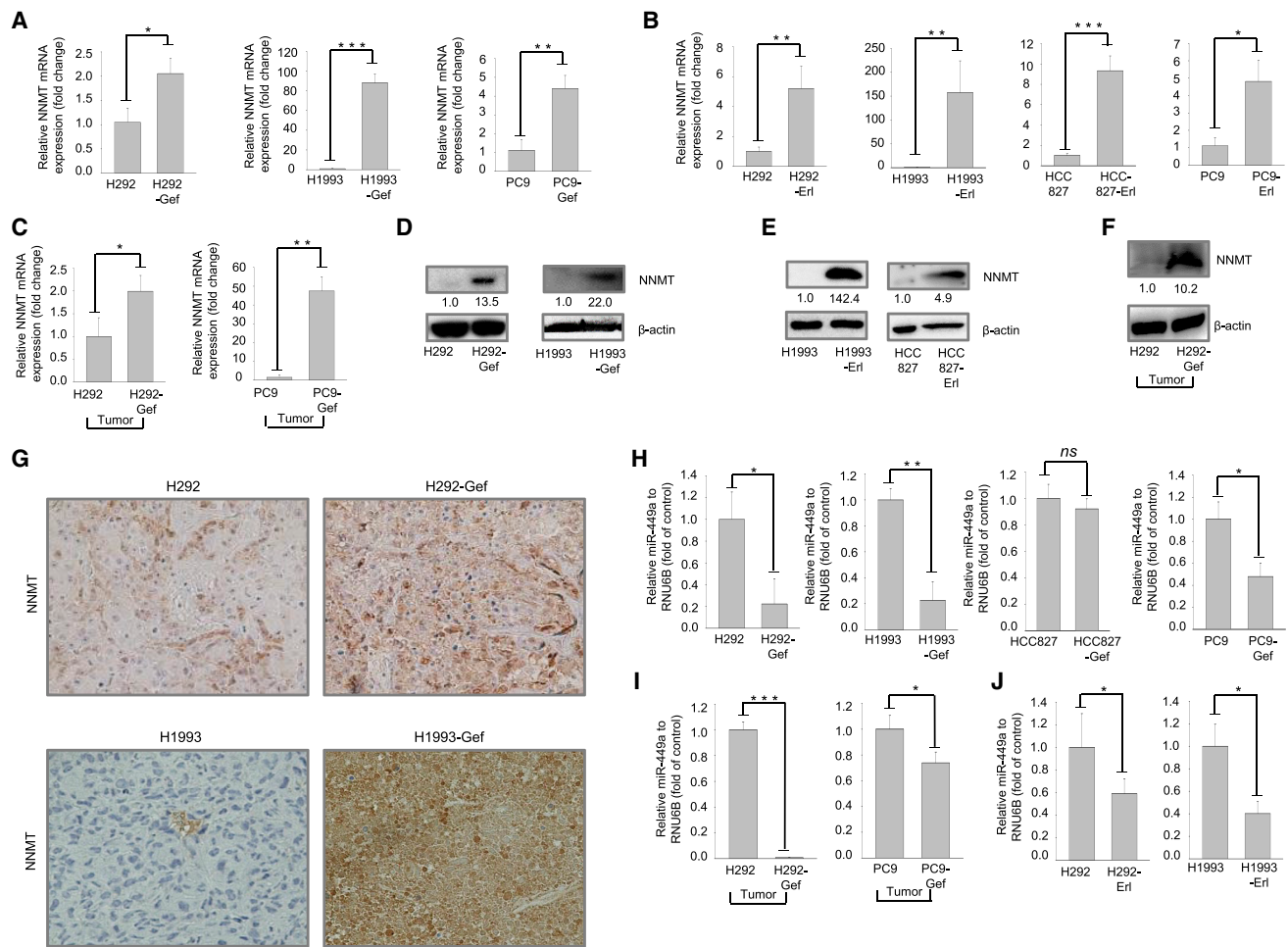
Figure 1. NNMT Expression Is Inversely Related to that of miR-449a in gef-Resistant NSCLC Tissues and Cell Lines

(A and B) Characterization of the indicated parental and gef-resistant phenotype cell lines (A) or erl-resistant phenotype cell lines for NNMT expression at mRNA levels (B). (C) Characterization of the indicated parental or gef-resistant phenotype tissues for NNMT expression at the mRNA levels. Total RNA was isolated and analyzed by real-time PCR using NNMT-specific primers and normalized to β-actin expression. (D and E) Confirmation of NNMT protein overexpression in gef-resistant cell lines (D) or erl-resistant cancer cell lines (E). (F) Confirmation of NNMT protein overexpression in gef-resistant tissues. The expression of NNMT protein was investigated by western blotting using β-actin as the loading control. (G) Immunohistochemistry of NNMT in tumor tissue sections. Immunohistochemical analysis of NNMT was performed using anti-NNMT antibody in tumor tissue sections. (H–J) Characterization of the indicated parental and gef-resistant cells (H) or erl-resistant cells (J) and tissues (I) for miR-449a expression. miR-449a levels were quantified by TaqMan real-time PCR and normalized to RNU6B. Data are representative of three independent experiments. *p < 0.05; **p < 0.01; ***p < 0.001 by the t test. *ns*, not significant.

Based on these findings, we sought to experimentally determine whether dual inhibition of NNMT by NNMT siRNA and miR-449a exhibited a synergistic antitumor efficacy. The combination of NNMT siRNA and miR-449a showed significantly different p values compared with each treatment of NNMT siRNA or miR-449a, particularly the combination index (CI) was 0.285 at Gef 10 μM (synergism), which led to a remarkable inhibition of cell proliferation in PC9-Gef cells (Figure 2H). Consequently, this combination was applied in additional functional studies. We found that *in vivo*, the miR-449a/siRNA NNMT (siNNMT) combination showed an enhanced antitumor activity compared with each treatment (Figure 2I; Figures S1E and S1F), without a significant change in body

weight (Figure S1G). We next examined the effects of dual therapy on antitumor activity in *in vivo* models. NNMT immunostaining and mRNA expression illustrated that the expression of NNMT was effectively suppressed after miR-449a and siNNMT treatment compared with the control (Figures S1H and S1I). We also confirmed the expression of miR-449a, which was highly upregulated compared with the control group *in vivo* (Figure S1J). Staining with Ki67, a biomarker of cell proliferation, also revealed that miR-449a or siNNMT suppressed the expression of Ki67, but the combination of miR-449a and siNNMT enhanced the suppression activity (Figure 2J). Taken together, the *in vitro* and *in vivo* data confirmed the improved therapeutic efficiency and antitumor activity of combined miRNA
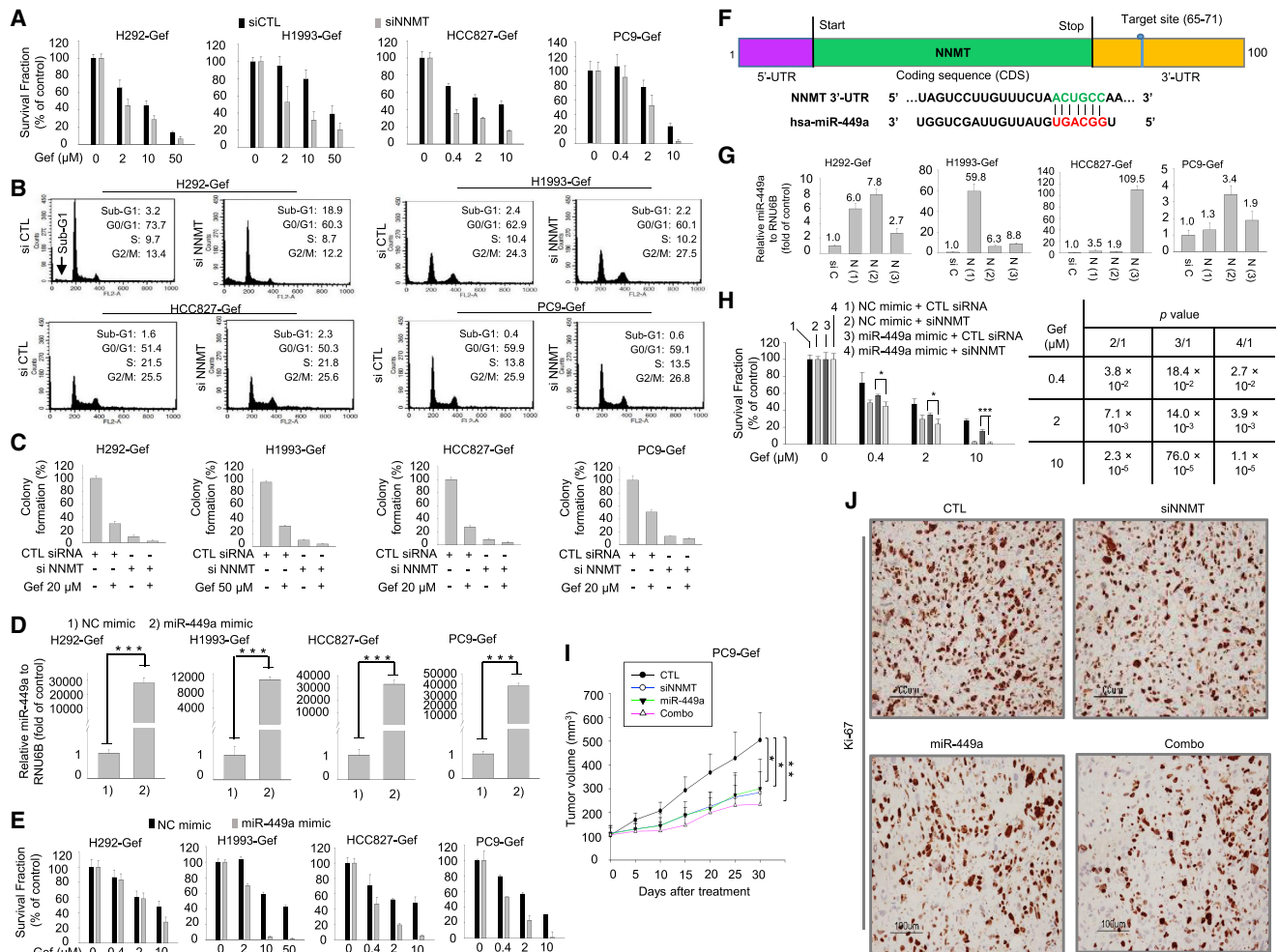
Figure 2. NNMT Stimulates gef-Resistant NSCLC Cell Growth by Targeting miR-449a

(A) Gefitinib sensitivity of the indicated gef-resistant phenotype cell lines. Cells were transiently post-transfected with scramble siRNA or NNMT siRNA for 48 hr and then incubated with the indicated concentrations of gef. Cell viability was assessed by the SRB assay. (B) Cell-cycle progression of gef-resistant phenotype cell lines. Cells were transiently transfected with either scramble siRNA or NNMT siRNA for 48 hr. Transfected cells were subjected to FACS analysis. (C) Colony formation of gef-resistant phenotype cell lines. Cells were transiently post-transfected with either scramble siRNA or NNMT siRNA for 48 hr and then cultured with the indicated concentrations of gef and subjected to colony formations assays. (D) Effects of miR-449a mimic on the miR-449a expression in gef-resistant cell lines. The indicated gef-resistant cell lines were cultured in six-well plates and then transfected with NC miRNA or miR-449a for 48 hr (50 pmol/well). The levels of miR-449a expression were determined by TaqMan real-time PCR with specific primers for mature miR-449a. Samples were normalized to RNU6B. (E) Gefitinib sensitivity of the indicated gef-resistant phenotype cell lines. Cells were transiently post-transfected with NC miRNA or miR-449a for 48 hr and then incubated with the indicated concentrations of gef. Cell viability was assessed by the SRB assay. (F) Bioinformatics analysis. The possible binding sites between NNMT and hsa-miR-449a were determined using a bioinformatics tool (http://www.targetscan.org/vert_71/). (G) Effects of siNNMTs on miR-449a expression by transfection with siNNMTs [N(1): siNNMT #1; N(2): siNNMT #2; N(3): siNNMT #3]. (H) Effects of siNNMT and/or miR-449a on cell proliferation by transfection with miR-449a and/or siNNMT in PC9-Gef cells. (I) Effects of miR-449a and/or siNNMT on tumor growth in PC9-Gef cells. (J) Immunohistochemistry of Ki-67 in tumor tissue sections. *p < 0.05; **p < 0.01; ***p < 0.001 by the t test.

and siRNA therapy compared with the individual treatments in gef-resistant cells.

Reversal of PTEN Promoter Methylation by miR-449a in Gef-Resistant NSCLC Cells

Phosphatase and tensin homolog (PTEN) plays an important role in cancer development and sensitivity to chemotherapy, and loss or decreased expression of PTEN has been correlated to acquired resis-tance.[11,25,26] While gef and erl, which target the EGFR, are approved for the treatment of patients with advanced NSCLC, PTEN loss is also associated with resistance to small-molecule EGFR inhibitors including gef.[27] A previous study reported that PTEN is downregu-lated in PC9-Gef compared with parental PC9 cells.[28] In the present study, we also confirmed and continuously investigated the expres-sion of PTEN in four cell lines with two different levels of EGFR-TKI resistance, including gef and erl. PTEN loss was observed in all

Table 1. Effects of Gefitinib on the Cell Proliferation of NSCLC Cells

	IC$_{50}$ of Gefitinib (μM)	
Cell Line	siCTL	siNNMT
H292-Gef	7.6	0.5
H1993-Gef	13.1	2.3
HCC827-Gef	3.9	0.4
PC-9-Gef	5.5	2.1
CTL, control.		

Table 2. Effects of Gefitinib on the Cell Proliferation of Resistance NSCLC Cells

	IC$_{50}$ of Gefitinib (μM)	
Cell Line	NC Mimic	miR-449a Mimic
H292-Gef	6.8	3.2
H1993-Gef	14.3	2.1
HCC827-Gef	2.7	0.3
PC-9-Gef	2.8	0.4

EGFR-TKI-resistant NSCLC cells by western blotting (Figure 3A) and confirmed by IHC analysis (Figure 3B).

Alternations in DNA methylation have been common and extensively studied in many cancers.[29] While Ulanovskaya et al.[2] found no significant NNMT-dependent changes in global cytosine, protein methylation was found to be markedly lower in cells with increased NNMT levels. Subsequently, 5-Aza-2'-deoxycytidine (5-Aza), a DNA methylation inhibitor, was employed to investigate its effect on PTEN and miR-449a. We found that 5-Aza suppressed the levels of NNMT protein expression (Figure 3C), while 5-Aza induced PTEN expression as reported previously[30,31] and stimulated the levels of miR-449a (Figure 3D). These data suggested that PTEN and miR-449a loss might be closely related to DNA methylation in gef-resistant NSCLC cells. Therefore, we further investigated the effect of miR-449a on PTEN promoter methylation, in which the promoter region contains the methylation site (Figure 3E, top panel).[32] The H292-Gef cells showed a significant downregulation of the expression level of miR-449a both *in vitro* and *in vivo* compared with the H292 cells employed in this study. Using EpiTect MethyLight assays, we found that miR-449a suppressed PTEN methylation, with approximately 3-fold changes compared with the control (Figure 3E, bottom right panel). Using methyl-specific PCR assays, we further confirmed that miR-449a induced PTEN un-methylation and suppressed PTEN methylation (Figure 3E, bottom left panel). These results indicated that miR-449a transduction was associated with aberrant methylation of the PTEN promoter site in gef-resistant NSCLC cells. Western blot analysis also revealed that miR-449a overexpression increased PTEN expression (Figure 3F).

Activation of the phosphatidylinositol 3-kinase (PI3K)/Akt pathway is reported to associate with drug resistance to chemotherapeutic drugs.[11,12] Therefore, targeting Akt might modulate the drug resistance in cancer cells.[33–35] The PI3K/Akt pathway was also previously reported to participate in NNMT-dependent MMP2 activation and cellular invasion.[7] Therefore, we further clarified the correlations between PTEN/PI3K/Akt and NNMT in gef-resistant NSCLC cells. Knockdown of PTEN (siPTEN) was found to increase the levels of p-Akt (Ser[473]) protein expression (Figure 3G). Employing LY294002, a PI3K inhibitor, we also observed suppression of NNMT in gef-resistant cells (Figure 3H). Next, we further elucidated the possible crosstalk between the miR-449a level and PI3K activity in gef-resistant NSCLC cells. We determined the levels of miR-449a in gef-resistant NSCLC cells in the presence of LY294002 and found that miR-449a expression was increased by PI3K inhibition (Figure 3I). We also found that knockdown of NNMT expression by treatment with NNMT siRNA decreased the levels of active Akt *in vitro* (Figure 3J) and *in vivo* (Figure 3K). In contrast, transfection with NNMT plasmid upregulated the levels of p-Akt in gef-resistant cells (Figure 3L). Taken together, these data raise the possibility that a positive feedback loop of miR-449a with NNMT and PI3K guarantees the sustained activation in the resistance of NSCLC cells, which is essential for the overexpression of NNMT.

YD Leads to Reversal of miR-449a and NNMT Expression in EGFR-TKI-Resistant NSCLC Cells

Based on the correlation between miR-449a and NNMT expression in resistant cancer cells, we assumed that an agent with the potential to reverse miR-449a and NNMT expression might be a drug candidate to overcome EGFR-TKI-resistant cancers. Natural products have emerged as an important source of agents in drug discovery and development.[18,19,36,37] Our previous study revealed that the expression of NNMT levels in H292-Gef was approximately 4.3-fold higher than that in H292 cells based on a cDNA array analysis.[21] Therefore, to confirm our hypothesis and explore the potential to overcome the resistance by regulating the expression of NNMT and miR-449a, we applied YD, a natural product-derived antitumor agent that was shown to be more sensitive to lung cancer cells compared with other solid cancer cell lines[20] (Table S1). As shown in Table 3, cDNA array analysis with the standard 2-fold change in expression as our threshold criterion revealed that NNMT was one of the most overexpressed genes in H292-Gef cells compared with H292 cells, and YD (10 nM) effectively suppressed the expression of NNMT with a 2.5-fold change. A subsequent analysis also confirmed that treatment with YD suppressed NNMT expression in gef-resistant NSCLC cells. YD downregulated the expression levels of NNMT protein, NNMT-related protein (p-Akt, Ser[473]), and NNMT mRNA in a concentration-dependent manner (Figures 4A and 4B). Interestingly, YD also effectively restored the decreased level of miR-449a in all gef-resistant cells in a concentration-dependent manner (Figure 4C).

In addition, the antitumor activity of YD was evaluated in nude mouse xenograft models implanted with MET amplification (H1993-Gef) and EGFR mutation (PC9-Gef) cell lines. As depicted
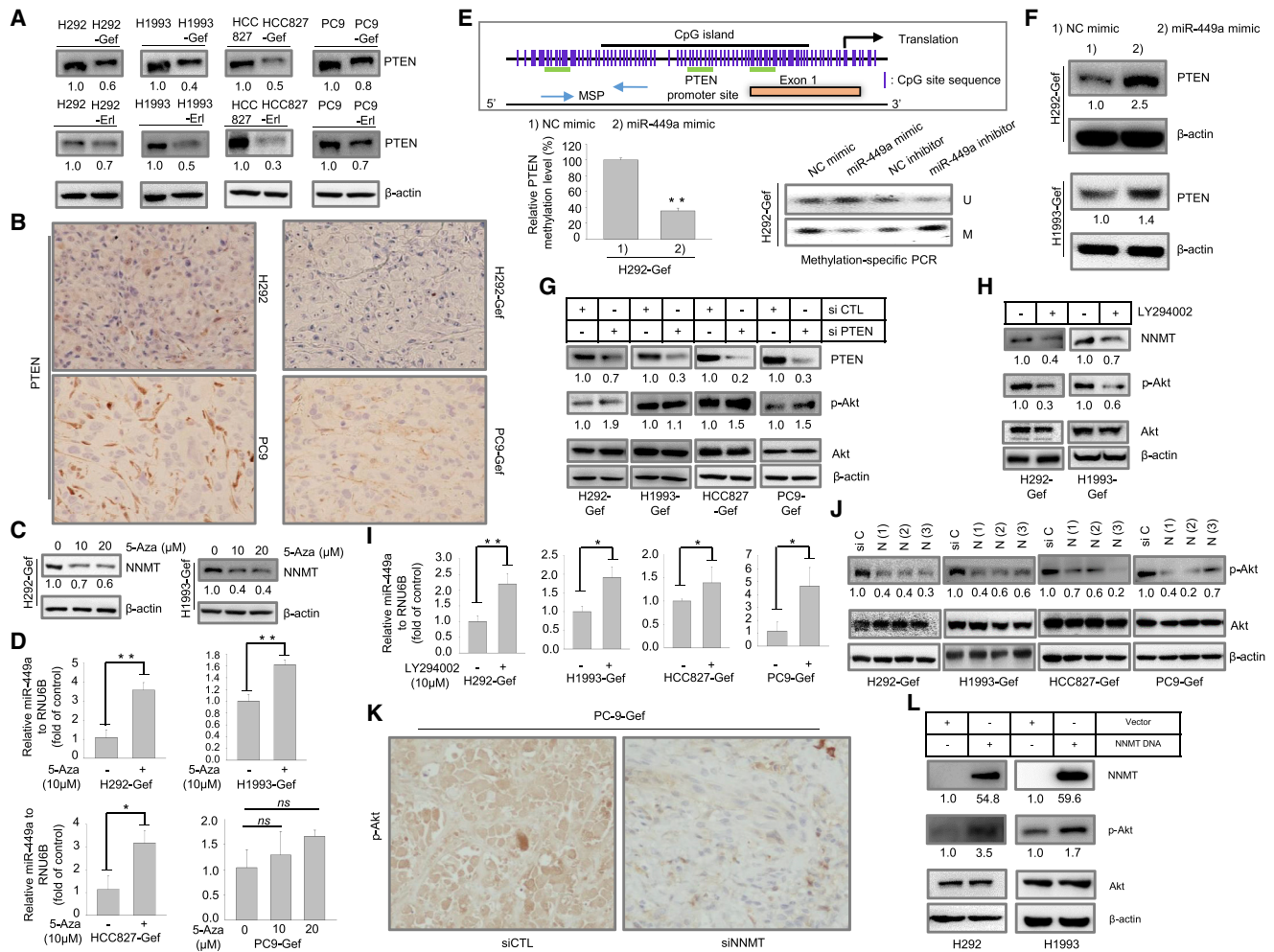
Figure 3. miR-449a Modulates the Growth of gef-Resistant NSCLC Cells through Induction of the PTEN Pathway

(A) Characterization of the indicated parental or drug-resistant phenotype cell lines for PTEN expression at protein levels. (B) Immunohistochemistry of PTEN in tumor tissue sections. Immunohistochemical analysis of PTEN was performed using anti-PTEN antibody in tumor tissue sections. (C and D) Effects of 5-Aza on the levels of NNMT (C) and miR-449a (D) expression. The drug-resistant cell lines were incubated in the presence or absence of 5-Aza (10 or 20 μM) for 24 hr. (E) Reversal of PTEN promoter methylation by miR-449a in gef-resistant cells. Top, methylation-specific PCR (MSP) analysis of the PTEN gene and map of the promoter region of the PTEN gene. Bottom, methylation-specific PCR analysis of the PTEN gene in H292-Gef cells. Bottom right, Cells were transfected with or without miR-449a (50 pmol/well) and furthered analyzed by using EpiTect MethyLight PCR kit as described in the Materials and Methods. Bottom left, Results of MSP analysis of PTEN gene in H292-Gef cells after post-transfection with or without miR-449a mimic and miR-449a inhibitor (50 pmol/well). M and U represent PCR products of methylated and unmethylated alleles, respectively. (F) Effects of miR-449a on the protein expression of PTEN. The gef-resistant cells were transfected with NC miR-449a or miR-449a for 48 hr. PTEN protein levels were determined from cell lysates by immunoblotting. (G) Effects of PTEN siRNA on the Akt pathway. The drug-resistant cell lines were incubated with scramble siRNA or PTEN siRNA for 48 hr and then analyzed by western blotting. (H) Effects of PI3K inhibitor on the Akt pathway. Cells were incubated with PI3K inhibitor (LY294002, 20 μM) for 24 hr and then analyzed by immunoblotting. (I) Effects of PI3K inhibitor on miR-449a. The gef-resistant cell lines were incubated with LY294002 for 24 hr; then the levels of miR-449a were determined using TaqMan real-time PCR. (J) Effects of NNMT siRNA on the Akt pathway. The gef-resistant cell lines were incubated with scramble siRNA or NNMT siRNA for 48 hr, and then the indicated protein levels were further analyzed by immunoblotting. (K) Immunohistochemistry of p-Akt in tumor tissue sections. Immunohistochemical analysis of p-Akt was performed using anti-p-Akt antibody in tumor tissue sections with or without NNMT siRNA. (L) Effects of NNMT plasmid on the Akt pathway. NNMT plasmid was transfected to the indicated parental cells within 48 hr; then further immunoblotting was performed to detect protein expressions. *p < 0.05; **p < 0.01; ***p < 0.001 by the t test. *ns*, not significant.

in Figures 4D, 4E, S2A, and S2B, YD (1 mg/kg) efficiently inhibited tumor growth in H1993-Gef and PC9-Gef cells, and was superior to gef in H1993-Gef and PC9-Gef cells without a significant change in body weight (Figures S2C and S2D). Interestingly, we also found that the suppression of NNMT by YD was higher than gef both

in vitro and *in vivo* (Figures 4F and 4G). IHC analysis confirmed that the expression of NNMT was suppressed in tumor tissues in the YD-treated groups (Figure 4H). In addition, YD was able to suppress NNMT mRNA expression in tumor tissues (Figure 4I) while concurrently inducing the levels of miR-449a expression (Figure 4J).

**Table 3. Effects of Yuanhuadine and Gefitinib on Gene Expression in H292-Gef Cells**

No.	Accession	FC (R CTL/H CTL)	FC (R YD/R CTL)	FC (R Gef/R CTL)	Gene Symbol	Description
1	NM_006169.2	+4.33	−2.55	–	NNMT	nicotinamide *N*-methyltransferase
2	NM_002543.3	+3.79	−2.31	–	OLR1	oxidized low-density lipoprotein (lectin-like) receptor 1
3	XM_034819.6	+2.39	−2.1	–	ZNF629	zinc-finger protein 629
4	NM_000600.1	+2.39	−3.3	–	IL6	interleukin-6 (interferon, beta 2)
5	NM_016352.2	+2.32	−3.41	–	CPA4	carboxypeptidase A4
6	NM_001360.2	+2.29	−2.34	–	DHCR7	7-dehydrocholesterol reductase
7	NM_003238.1	+2.21	−2.1	–	TGFB2	transforming growth factor, beta 2
8	NM_005585.3	+2.07	−3.63	–	SMAD6	SAMD family member 6
1	NM_002575.1	−21.64	+20.75	−2.69	SERPINB2	serpin peptidase inhibitor, clade B (ovalbumin), member 2
2	NM_007036.3	−6.79	+3.69	–	ESM1	endothelial cell-specific molecule 1
3	NM_198129.1	−6.45	+4.82	–	LAMA3	laminin, alpha 3
4	NM_005554.3	−5.62	+3.98	–	KRT6A	keratin 6A
5	NM_139314.1	−4.82	+2.75	−3.28	ANGPLT4	angiopoietin-like 4
6	NM_005562.1	−4.32	+3.41	–	LAMC2	laminin, gamma 2
7	NM_004029.2	−4.15	+2.17	–	IRF7	interferon regulatory factor 7
8	NM_000024.4	−4.08	+2.5	–	ADRB2	adrenergic, beta-2 receptor
9	NM_000240.2	−3.84	+3.84	–	MAOA	monoamine oxidase A
10	NM_000963.1	−3.83	+5.65	−3.01	PTGS2	prostaglandin-endoperoxide synthase 2
11	NM_006850.2	−3.76	+15.87	−3.3	IL24	interleukin-24
12	NM_058172.3	−3.29	+2.77	–	ANTXR2	anthrax toxin receptor 2
14	NM_002658.2	−2.84	+10.67	–	PLAU	plasminogen activation urokinase
15	NM_173343.1	−2.73	+6.67	–	IL1R2	interleukin-1 receptor, type II
16	NM_000584.2	−2.63	+4.99	−3.84	IL8	interleukin-8
17	NM_031892.1	−2.62	+2.34	–	SH3KBP1	SH3-domain kinase binding protein 1
18	NM_005555.3	−2.45	+4.11	–	KRT6B	keratin 6B
19	NM_002203.3	−2.42	+4.95	−2.07	ITGA2	integrin, alpha 2
20	NM_005863.3	−2.35	+2.52	–	NET1	neuroepithelial cell transforming 1
21	NM_005318.2	−2.32	+2.56	–	H1F0	H1 histone family, member 0
22	NM_002153.1	−2.26	+6.99	–	HSD17B2	hydroxysteroid (17-beta) dehydrogenase 2
23	NM_001109.3	−2.26	+3.77	−2.63	ADAM8	ADAM metallopeptidase domain 8
25	NM_000228.2	−2.21	+2.17	–	LAMB3	laminin, beta 3
26	NM_006238.3	−2.21	+3.54	–	PPARD	peroxisome proliferative-activated receptor, delta
27	NM_004431.2	−2.17	+2.31	−2.07	EPHA2	EPH receptor A2
28	NM_004029.2	−2.07	+2.17	–	IRF7	interferon regulatory factor 7
29	NM_014631.2	−2.07	+2.47	–	SH3PXD2A	SH3 and PX domains 2A
30	NM_000611.4	−2.02	+2.28	–	CD59	CD59 molecule, complement regulatory protein
31	NM_006244.2	−2.01	+2.51	–	PPP2R5B	protein phosphatase 2, regulatory subunit B, beta isoform

The effects of 10 nM yuanhuadine and 50 nM gefitinib on gene expression in H292-Gef cells are listed. +, upregulated; −, downregulated; CTL, control; FC, fold change; Gef, gefitinib; H, H292; R, H292-Gef; YD, yuanhuadine.

Taken together, these findings were consistent with the changes in expression of miR-449a and NNMT *in vitro*, suggesting that both YD and miR-449a could regulate the expression of NNMT and indeed could be useful for the suppression of NNMT overexpression, which could lead to improved sensitivity of gef in gef-resistant cancer cells.

YD Suppresses NNMT Activity via the Interacting Pocket of the Enzyme

To date, there have been very few reports about NNMT inhibitors, especially from natural products. Herein, in an effort to identify the interactions between YD and NNMT, the ability of YD to inhibit NNMT enzyme activity was initially determined using a biochemical
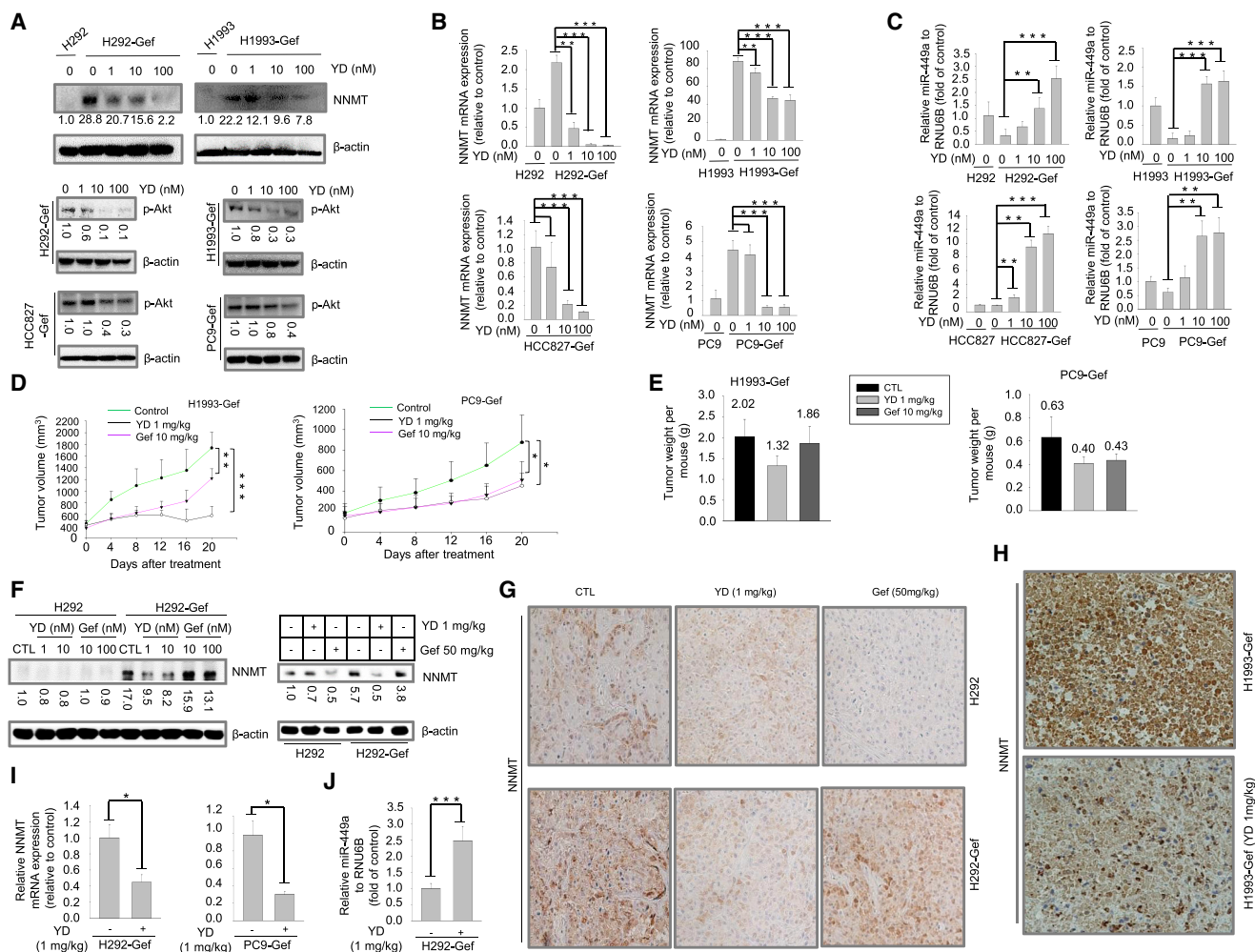
Figure 4. YD Regulates miR-449a and NNMT Overexpression in gef-Resistant NSCLC Cells

(A) Effects of YD on NNMT and the related protein expression. NNMT, p-Akt, Akt, and β-actin protein levels in cell lysates were assayed by immunoblotting after 24 hr of YD treatment. (B) Effects of YD on NNMT mRNA expression. NNMT mRNA expression was evaluated by real-time PCR after 24 hr of YD treatment. (C) Effects of YD on miR-449a expression. miR-449a levels were further analyzed using the TaqMan PCR kit after 24 hr of YD treatment. (D) The indicated cells were implanted subcutaneously into the flanks of BALB/c nude mice. Dosing of YD (1 mg/kg body weight) or gef (10 mg/kg body weight) was initiated when the tumor volumes reached approximately 400 mm^3 for H1993-Gef cells or 150 mm^3 for PC9-Gef cells. YD and gef were administrated orally once daily for 21 days continuously. The tumor volumes were measured every 4 days (n = 5 mice per group). The error bars represent the means ± SD. (E) H1993-Gef and PC9-Gef tumors were excised from animals on day 21 after treatment, and tumor weights were calculated. (F) Protein expression levels of NNMT. The proteins from cell lysates (right panel) or small portions of tumors from each group were homogenized in Complete Lysis Buffer (Active Motif) (left panel) for immunoblotting. β-Actin was used as an internal standard. (G and H) Immunohistochemistry of NNMT in tumor tissue sections of H292 and H292-Gef (G) or H1993-Gef (H). Immunohistochemical analysis of NNMT was performed using anti-NNMT antibody in each of the indicated groups. (I and J) Relative expression of NNMT and miRNA-449a in tumor transcripts of the indicated xenograft tissues. The levels of NNMT (I) or miR-449 (J) expression were analyzed by real-time PCR or with the TaqMan PCR kit using specific primers, respectively. *p < 0.05; **p < 0.01; ***p < 0.001 by the t test.

in vitro assay. The analysis revealed an inhibitory activity of the NNMT enzyme by YD with an IC$_{50}$ of 0.4 μM. As a positive control, 1-MNA was used for *in vitro* NNMT inhibition (Figure 5A). To understand the potential interactions of YD in the binding site of NNMT, we used the published crystal structure of human NNMT complexed with SAH and NCA for the docking study (pdb:3ROD). Due to the low similarity between the original ligands (SAH and NCA) and YD, the majority of the interactions observed in the original pdb structure (Figure 5B) were changed. The structure of the

NNMT-YD complex with the highest docking score is shown in Figure 5C. YD, which possesses 10 oxygen atoms including three hydroxyl groups, exhibits several hydrogen bonds and van der Waals interactions with NNMT in the binding site. Hydrogen bonds were observed between: (1) the acetyl group of YD and the hydroxyl group of Tyr20; (2) the hydroxyl group of YD and the backbone amide of Tyr86, as well as the side chain of Asn90; (3) the primary alcohol of YD and the side chain amide of Gln89; and (4) the oxygen atom of the dioxolane ring and the hydroxyl group of Tyr204. Among
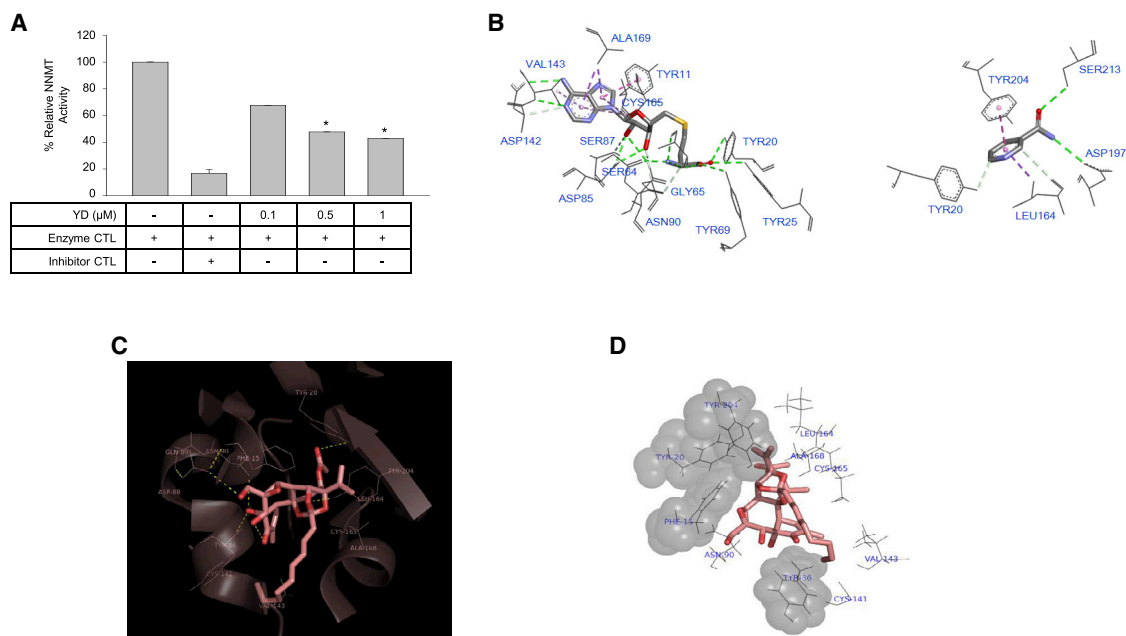
Figure 5. YD Interacts with the Binding Site of NNMT

(A) *In vitro* activity of purified NNMT was assessed in the presence of increasing concentrations of YD. Data are reported as a percentage of NNMT activity with respect to the control. Histograms represent the mean ± SD of three independent experiments. (B) Binding site of hNNMT complexed with *S*-adenosylhomocysteine (SAH) and nicotinamide (NCA). (C) Docked pose of YD with the highest binding score. Hydrogen bonds within the binding site are shown as yellow lines. (D) Residues forming hydrophobic interactions with YD are shown as gray lines. Among them, previously reported conserved aromatic residues (Phe15, Tyr20, Tyr86, and Tyr204) are presented as spheres. *$p < 0.05$.

them, the interaction with Tyr20 was an important element for the reported ligand (SAH).[38] Residues with hydrophobic interactions are shown in Figure 5D. A portion of the clustered conserved aromatic residues (Phe15, Tyr20, Tyr86, and Tyr204) reported previously are shown in spheres.[38] Tyr86, which interacted with the adenine ring in the original structure, displayed a pi-alkyl interaction with the alkyl side chain of YD. Tyr204 and Leu164, residues that form a sandwiched hydrophobic interaction for the NCA ring, exhibited pi-alkyl and alkyl hydrophobic interactions with the propylene group of YD, respectively.

DISCUSSION

Clinically, advanced NSCLC patients who suffer EGFR-TKI resistance currently have limited therapeutic options. Improved detection methods for cancer diagnosis are crucial for early and reliable prognosis and treatment.[39] Therefore, molecular profiling and gene expression analysis are considered useful tools for improving outcomes and minimizing side effects. We investigated the expression profiles of NNMT and miR-449a and their possible interactions both *in vitro* and *in vivo* in EGFR-TKI-resistant NSCLC cells. The association between miR-449a and c-MET expression has also been previously elicited in sunitinib-resistant renal cell carcinoma,[23] and amplification of c-MET has been implicated in resistance to therapies targeting the EGFR.[40] In the present study, we observed that the NNMT protein and mRNA were overexpressed, while miR-449a was significantly downregulated in EGFR-TKI-resistant NSCLC cells

compared with their parental cells, especially with H1993, a high-c-MET-expressing NSCLC cell line. Subsequently, further study about the plausible association between MET amplification and NNMT/miR-449a expression can be potentially needed. We further employed bioinformatics tools and found possible correlations between NNMT and miR-449a. Moreover, knockdown of NNMT induced the expression of miR-449a in drug-resistant NSCLC cells. These findings suggested that the mechanism underlying the miR-449a downregulation might be related to the upregulated NNMT expression in resistant NSCLC cells. It is possible that NNMT-mediated downregulation of miR-449a is impaired in drug-resistant cancer cells.

The regulation of PTEN expression is a critical strategy for therapeutic sensitivity, and its dysregulation is often associated with cancer drug resistance. Our group has newly described a significant function of PTEN in regulating tumor progression.[11] Moreover, variation in NNMT enzyme activity could lead to toxicological and pharmacological consequences. In fact, methylation is a fundamental process in the biotransformation of many drugs and xenobiotic compounds, and NNMT, which catalyzes the *N*-methylation of pyridines that are structurally related to NCA, has a primary role in detoxifying many xenobiotics.[2] Therefore, we employed 5-Aza, a methylation inhibitor, and found that it suppressed NNMT expression while inducing the expression of miR-449a in gef-resistant NSCLC cells. This finding led us to investigate the methylation status of the PTEN promoter in miR-449a-overexpression resistant NSCLC cells.

The overexpression of miR-449a was able to suppress the methylation intensity of the PTEN promoter and restore the expression of PTEN in EGFR-TKI-resistant NSCLC cells. This result suggests that miR-449a-dominated NNMT expression is crucial for PTEN expression in drug-resistant NSCLC cells. In addition, PTEN may also exert its role as a tumor suppressor by negatively regulating the PI3K/Akt pathway, which determines cell growth, survival, and inhibition in both cancer and normal cells.[41,42] Thereby, we further employed LY294002, a PI3K inhibitor, and found that PI3K suppression by LY294002 treatment suppressed NNMT expression and also restored the expression of miR-449a in gef-resistant NSCLC cells. These results imply that constitutive activation of the PI3K/Akt pathway is also involved in the control of miR-449a-mediated NNMT expression in the resistance of NSCLC cells. Hence, a positive feedback loop between the PTEN-controlled PI3K/Akt pathway and miR-449a-mediated NNMT expression in drug resistance of NSCLC cells seems to be crucial for the enhanced cell proliferation and decreased gef sensitivity.

Although the role of NNMT in drug resistance has been emerging, there are few reports of NNMT inhibitors in cancer cells. Employing cDNA analysis with YD and *in vitro* results, we found that the downregulation of NNMT by YD enhanced the sensitivity of gef in gef-resistant cells. We also found that the expression of miR-449a could be significantly upregulated by YD, suggesting that the growth of gef-resistant NSCLC cells could be reverted by treating EGFR-TKI-resistant NSCLC cells with YD. This significant point could be exploited for the future design of novel strategies for the prevention of tumor progression and/or treatment of lung cancer using the combination of YD and miR-449a. Although studies of the interactions between YD and NNMT are limited, we revealed interactions between the active sites of this enzyme with YD. Further analyses of NNMT and YD interactions will be essential to design and develop new NNMT inhibitors.

In summary, we suggest that the overexpression of NNMT in gef-resistant cells is caused by the deregulation of its positive feedback loop between the PTEN/PI3K/Akt pathway and miR-449a. In addition, we confirmed that YD, a natural antitumor agent, is able to overcome the resistance via modulation of NNMT and miR-449a in NSCLC. These findings indicate that targeting the NNMT overexpression mechanism might be a novel therapeutic strategy in EGFR-TKI-resistant NSCLC patients.

MATERIALS AND METHODS

Reagents

RPMI 1640 medium and Opti-MEM Reduced Serum Medium were purchased from Invitrogen (CA, USA). Mouse anti-β-actin and anti-NNMT (G-4) were purchased from Santa Cruz Biotechnology (Santa Cruz, CA, USA). Rabbit anti-Akt, anti-phospho-Akt (Ser473), and anti-PTEN were purchased from Cell Signaling Technology (Danvers, MA, USA). YD (purity > 98.5%) was isolated and identified from a $CHCl_2$-soluble fraction of the flowers of *Daphne genkwa*, as described previously.[19,20]

Cell Culture and Establishment of EGFR-TKI Resistance of NSCLC Cells

Human lung carcinoma H292 and H1993 cells were obtained from the American Type Culture Collection (Manassas, VA, USA). The cell lines were cultured in RPMI 1640 medium supplemented with 10% FBS and antibiotics-antimycotics (PSF; 100 U/mL penicillin G sodium, 100 μg/mL streptomycin, and 250 ng/mL amphotericin B). gef-resistant H292 (H292-Gef) cells were developed by our group as described previously,[19] while erl-resistant H292 (H292-Erl) cells were developed from the parental H292 cells through continuous exposure to gradually increasing concentrations of erl (Selleckchem, Houston, TX, USA) and maintained in RPMI 1640 medium containing 1 μM erl. Similarly, to establish gef-resistant H1993 cells (H1993-Gef) and erl-resistant H1993 cells (H1993-Erl), we continuously exposed H1993 cells to increasing drug doses up to 10 μM gef and erl. Subsequently, H1993 cells with established resistance were maintained in medium containing 10 μM gef and erl. All cells were incubated at 37°C in a humidified atmosphere containing 5% CO_2 and sub-cultured at least twice a week. Cells passaged more than three times were used for the experiments as described previously.[36]

Transfection of siRNAs and MicroRNA

The siRNA sequences (Stealth RNAi siRNA; Invitrogen) targeting NNMT (siNNMT-1: Cat. No. HSS181544, siNNMT-2: Cat. No. HSS107222, siNNMT-3: Cat. No. HSS107223), the negative control (NC) (Negative Universal Control Med Cat. No. 46-2001), the miR-449a mimic (mirVana miRNA Mimic, assay ID MC11127), and the NC (mirVana miRNA Mimic NC No. 1; Applied Biosystems) were transfected into the cell lines by electroporation using Lipofectamine RNAiMAX (Invitrogen, CA, USA) according to the manufacturer's recommendations. The cells were harvested for subsequent experiments 24 and 48 hr post-transfection for real-time PCR and western blot analysis, respectively.

RNA Extraction and Real-Time PCR

RNA extraction and real-time PCR were carried out similarly as described previously.[36,43] Gene-specific primers for real-time PCR were synthesized by Bioneer Corporation (Daejeon, Korea): human NNMT sense: 5′-TGTGTGATCTTGAAGGGAACAG-3′, antisense: 5′-CTTGACCGCCTGTCTCAAC-3′; human β-actin sense: 5′-AGCA CAATGAAGATCAAGAT-3′, antisense: 5′-TGTAACGCAACTAAG TCATA-3′.

Plasmid Transfection

FuGENE HD Transfection Reagent (Roche Applied Science) was used to transfect plasmid pcDNA™3.1(+)-NNMT (#RG200641; Origene) or pCMV6-AC-GFP (#PS 100010) control vector into parental NSCLC cells. All transfections procedures were performed according to the protocol provided by the manufacturer. After transfection for 48 hr, NSCLC cells were harvested and extracted for protein isolation.

miRNA qPCR

To determine the expression of miR-449a in NSCLC cells, we used the TaqMan MiRNA Assay kit (Cat. No. 4427975; Applied Biosystems)

following the manufacturer's protocol. In detail, miRNA expression was determined by collecting total RNA from 90% confluent cells. Total RNA was isolated using TRIzol (Invitrogen, CA, USA) and then converted to cDNA using the TaqMan MiRNA Assay (Part No. 4366596) according to the manufacturer's protocol. The specific primer for mature miRNA was hsa-miR-449a (5′-UGGCAGUG UAUUGUUAGCUGGU-3′). The miR-449a (Assay ID: 001030) expression levels were analyzed using TaqMan real-time qPCR (TaqMan MicroRNA Assay; Applied Biosystems) and normalized to the RNU6B, an endogenous control (Assay ID: 001093). All reactions were performed in triplicate.

Cell Proliferation Assay
The cell proliferation assay was carried out similarly as described previously.[36]

Flow Cytometry for Cell-Cycle Analysis
The indicated cells were post-transfected with either scramble siRNA or NNMT siRNA for 48 hr; then the transfected cells were subjected to fluorescence-activated cell sorting (FACS) analysis as described previously.[36]

Analysis of Drug Combination
The cells were post-transfected with siNNMT and/or miR-449a and their scramble siRNA and/or NC miRNA; then the transfected cells were determined using the SRB assay. The combination effect was evaluated as described previously,[19] and the CI values were compared with the reference values reported by Chou.[44]

Western Blot Analysis
Immunoblotting analysis was performed according to previously published procedures.[36,43]

Methylation-Specific PCR
The methylation status of the PTEN promoter was determined by methylation-specific PCR after bisulfite-modification. The methylation sites of the PTEN gene promoter involved region sites MF (5′-TTCGTTCGTCGTCGTCGTATTT-3′), MR (5′-GCC GCTTAACTCTAAACCGCAA-3′), UF (5′-GTGTTGGTGGAGG TAGTTGTTT-3′), and UR (5′-ACCACTTAACTCTAAACCA CAACCA-3′). Genomic DNA was isolated and modified by bisulfite using an EpiTect Bisulfite kit (QIAGEN, Valencia, CA, USA). The EpiTect MethyLight PCR kit (Cat. No. 59496; QIAGEN, Valencia, CA, USA) was then employed for quantitative real-time probe-based PCR analysis of methylation status. Methylated and un-methylated genomic regions can be amplified by PCR using each sequence-specific pair of primers.

NNMT Enzyme Assay
The NNMT enzyme activity was measured using S-adenosyl methionine (SAM) as the methyl group donor and NCA as the substrate from Biovision (Cat No. K822-100; Milpitas, CA, USA) according to the manufacturer's instructions.

5-Aza Treatment
A stock solution of 10 mM 5-Aza obtained from Sigma was prepared in DMSO. H292-Gef, H1993-Gef, HCC-Gef, and PC-9-Gef cells were treated for 24 hr with 10 μM 5-Aza, and total protein or RNA was extracted for western blotting or qRT-PCR, respectively.

Colony Formation Assay
Resistant NSCLC cells were plated in a 35-mm culture dish at a density of 100 cells/dish. Twenty-four hours later, fresh medium containing NNMT siRNA or control siRNA was added to culture dishes. Forty-eight hours post-transfection with NNMT siRNA, the cells were washed with PBS or treated with gef for an additional 24 hr and allowed to grow in plasmid-free medium for 14 days (37°C, 100% humidity, 5% CO_2 atmosphere). Cell colonies were fixed with 2% paraformaldehyde (PFA), stained with crystal violet (0.5% w/v), and then counted visually or by using ImageJ software. The percentage of cells surviving the treatment relative to solvent-treatment controls was calculated.

cDNA Microarray Expression Analysis
The cDNA array was continuously employed as described previously[21] to analyze and compare H292-Gef cells treated with YD (10 nM) and non-treated H292-Gef cells.

In Vivo Tumor Xenograft Model
All animal experiments and care were conducted in a manner that conformed to the Guidelines of the Institutional Animal Care and Use Committee at Seoul National University and were approved by the Korean Association of Laboratory Animal Care (Permission No. SNU-161117-1).

For the nucleic acid in vivo study, miR-449a, control miRNA, siNNMT, and control siRNA were purchased from Bioneer Corporation (Daejeon, Korea). These miRNAs and siRNAs were conjugated to in vivo-jetPEI transfection reagent (Polyplus-transfection, New York, NY, USA) according to the manufacturer's instructions. Male mice aged 4–6 weeks were purchased from the National Laboratory Animal Centre. These mice received 200 μL of subcutaneous transplants that consisted of 1×10^7 cells of PC-9-Gef. On day 14 post-implantation, the mice were randomly divided into four groups (n = 5 per group): (1) control miRNA + control siRNA, (2) control miRNA + siNNMT, (3) control siRNA + miR-449a, and (4) miR-449a + siNNMT treated with multipoint intratumoral injection (10 μg per 100 μL per tumor for siRNAs two times per week and 20 μg per 100 μL per tumor for miRNAs three times per week) of these nucleic acids complexed with in vivo-jetPEI in 5% glucose for 3 weeks. After completion of the treatment over 1 additional week, the mice were sacrificed, and the mouse weight, tumor weight, number of nodules, and distribution of the tumors were recorded.

H1993-Gef and PC9-Gef cells were injected subcutaneously into the flanks of the mice (1×10^7 cells in 200 μL of medium), and tumors were allowed to grow. When the tumor volume reached approximately 400 mm^3 (H1993-Gef) and 150 mm^3 (PC9-Gef), the mice were

randomized into vehicle control and treatment groups (n = 5). YD (1 mg/kg), or Gef (10 kg/mg) dissolved in a volume of 150 μL of vehicle solution (Tween 80-ethanol-H_2O, 1:1:98) was administrated orally once a day for 22 days. The control group was treated with an equal volume of vehicle. The tumor volume was monitored two times per week for 22 days using calipers and estimated using the following formula: tumor volume (mm^3) = (width) × (length) × (height) × $\pi/6$. The body weight of each mouse was also monitored for toxicity.

Immunohistochemistry of Human Cancer Tissues
The excised tumors were fixed in 4% PFA and embedded in paraffin. Sectioned slides of the embedded specimens were serially deparaffinized, and the samples were rehydrated and subjected to antigen retrieval. The slides were incubated overnight with the indicated antibody at 4°C. After washing with PBS, the sections were incubated with HRP-conjugated anti-rabbit IgG for 30 min, washed with PBS, and then detected using the LSAB+ System-HRP kit from Dako (Glostrup, Denmark) and counterstained with H&E. Finally, the stained sections were observed and photographed under an inverted phase-contrast microscope.

Ex Vivo Biochemical Analysis of Tumors
A portion of frozen tumors excised from each nude mouse was thawed on ice and homogenized using a hand-held homogenizer in Complete Lysis Buffer (Active Motif, Carlsbad, CA, USA). Aliquots were stored at −80°C, and the expression of protein, mRNA, and miRNA levels of the tumor lysates were determined.

Molecular Docking Analysis
Molecular docking simulation was carried out using the SYBYL-X2.1.1 (Tripos, St. Louis, MO, USA) with Surflex-Dock Geom mode. The chemical structure of YD was prepared in a mol2 format, and the ligand was docked into chain A of the human NNMT downloaded from the PDB (PDB: 3ROD). Staged minimization was performed using Powell's method until the gradient converged to a value of 0.001 kcal/mol·Å. An MMFF94 force field was used with MMFF94 charges. Protomol was generated based on the location of the original ligands, SAH and NCA, with a threshold of 0.5 Å and bloat of 6 Å. The protein movement option was used to allow flexibility in the binding pocket of the protein. Docking performance was validated based on the docking scores, visual inspection, and root-mean-square deviation (RMSD) values of the re-docked poses compared with the original structure. Molecular interactions between the ligand and protein were further analyzed using the Discovery studio 4.0 Visualizer (Biovia, San Diego, CA, USA) or PyMOL-v1.0 (Schrödinger KK, Tokyo, Japan).

Statistical Analysis
Data are expressed as means ± SD for the indicated number of independently performed experiments. Student's t test or one-way ANOVA followed by Newman-Keuls multiple comparison test were used to examine between-group differences. Statistical significance was accepted at either $p < 0.05$, $p < 0.01$, or $p < 0.001$ (ns indicates not significant). Data analyses were performed using GraphPad Prism (Version 6).

CONFLICTS OF INTEREST
No potential conflicts of interest were disclosed.

REFERENCES

1. Zhao, D.P., Yang, C.L., Zhou, X., Ding, J.A., and Jiang, G.N. (2014). Association between CLPTM1L polymorphisms (rs402710 and rs401681) and lung cancer susceptibility: evidence from 27 case-control studies. Mol. Genet. Genomics 289, 1001–1012.

2. Ulanovskaya, O.A., Zuhl, A.M., and Cravatt, B.F. (2013). NNMT promotes epigenetic remodeling in cancer by creating a metabolic methylation sink. Nat. Chem. Biol. 9, 300–306.

3. Roessler, M., Rollinger, W., Palme, S., Hagmann, M.L., Berndt, P., Engel, A.M., Schneidinger, B., Pfeffer, M., Andres, H., Karl, J., et al. (2005). Identification of nicotinamide N-methyltransferase as a novel serum tumor marker for colorectal cancer. Clin. Cancer Res. 11, 6550–6557.

4. Zhu, H., Wu, H., Liu, X., Evans, B.R., Medina, D.J., Liu, C.G., and Yang, J.M. (2008). Role of MicroRNA miR-27a and miR-451 in the regulation of MDR1/P-glycoprotein expression in human cancer cells. Biochem. Pharmacol. 76, 582–588.

5. Yu, T., Wang, Y.T., Chen, P., Li, Y.H., Chen, Y.X., Zeng, H., Yu, A.M., Huang, M., and Bi, H.C. (2015). Effects of nicotinamide N-methyltransferase on PANC-1 cells proliferation, metastatic potential and survival under metabolic stress. Cell. Physiol. Biochem. 35, 710–721.

6. Kim, J., Hong, S.J., Lim, E.K., Yu, Y.S., Kim, S.W., Roh, J.H., Do, I.G., Joh, J.W., and Kim, D.S. (2009). Expression of nicotinamide N-methyltransferase in hepatocellular carcinoma is associated with poor prognosis. J. Exp. Clin. Cancer Res. 28, 20.

7. Tang, S.W., Yang, T.C., Lin, W.C., Chang, W.H., Wang, C.C., Lai, M.K., and Lin, J.Y. (2011). Nicotinamide N-methyltransferase induces cellular invasion through activating matrix metalloproteinase-2 expression in clear cell renal cell carcinoma cells. Carcinogenesis 32, 138–145.

8. Holohan, C., Van Schaeybroeck, S., Longley, D.B., and Johnston, P.G. (2013). Cancer drug resistance: an evolving paradigm. Nat. Rev. Cancer 13, 714–726.

9. Migliore, C., and Giordano, S. (2013). Resistance to targeted therapies: a role for microRNAs? Trends Mol. Med. 19, 633–642.

10. Engelman, J.A., and Settleman, J. (2008). Acquired resistance to tyrosine kinase inhibitors during cancer therapy. Curr. Opin. Genet. Dev. 18, 73–79.

11. Bach, D.-H., Hong, J.-Y., Park, H.J., and Lee, S.K. (2017). The role of exosomes and miRNAs in drug-resistance of cancer cells. Int. J. Cancer 141, 220–230.

12. Bach, D.-H., and Lee, S.K. (2018). Long noncoding RNAs in cancer cells. Cancer Lett. 419, 152–166.

13. Liu, J., Valencia-Sanchez, M.A., Hannon, G.J., and Parker, R. (2005). MicroRNA-dependent localization of targeted mRNAs to mammalian P-bodies. Nat. Cell Biol. 7, 719–723.

14. Saxena, S., Jónsson, Z.O., and Dutta, A. (2003). Small RNAs with imperfect match to endogenous mRNA repress translation. Implications for off-target activity of small inhibitory RNA in mammalian cells. J. Biol. Chem. 278, 44312–44319.

15. Weir, H.M., Bradbury, R.H., Lawson, M., Rabow, A.A., Buttar, D., Callis, R.J., Curwen, J.O., de Almeida, C., Ballard, P., Hulse, M., et al. (2016). AZD9496: an oral estrogen receptor inhibitor that blocks the growth of ER-positive and ESR1-mutant breast tumors in preclinical models. Cancer Res. 76, 3307–3318.

16. Yu, Z.Y., Xiao, H., Wang, L.M., Shen, X., Jing, Y., Wang, L., Sun, W.F., Zhang, Y.F., Cui, Y., Shan, Y.J., et al. (2016). Natural product vibsanin A induces differentiation of myeloid leukemia cells through PKC activation. Cancer Res. 76, 2698–2709.

17. Bachegowda, L., Morrone, K., Winski, S.L., Mantzaris, I., Bartenstein, M., Ramachandra, N., Giricz, O., Sukrithan, V., Nwankwo, G., Shahnaz, S., et al. (2016). Pexmetinib: a novel dual inhibitor of Tie2 and p38 MAPK with efficacy in preclinical models of myelodysplastic syndromes and acute myeloid leukemia. Cancer Res. 76, 4841–4849.

18. Kim, W.K., Bach, D.-H., Ryu, H.W., Oh, J., Park, H.J., Hong, J.-Y., Song, H.H., Eum, S., Bach, T.T., and Lee, S.K. (2017). Cytotoxic activities of Telectadium dongnaiense and its constituents by inhibition of the Wnt/β-catenin signaling pathway. Phytomedicine 34, 136–142.

19. Bae, S.Y., Hong, J.Y., Lee, H.J., Park, H.J., and Lee, S.K. (2015). Targeting the degradation of AXL receptor tyrosine kinase to overcome resistance in gefitinib-resistant non-small cell lung cancer. Oncotarget 6, 10146–10160.

20. Hong, J.Y., Chung, H.J., Lee, H.J., Park, H.J., and Lee, S.K. (2011). Growth inhibition of human lung cancer cells via down-regulation of epidermal growth factor receptor signaling by yuanhuadine, a daphnane diterpene from Daphne genkwa. J. Nat. Prod. 74, 2102–2108.

21. Bae, S.Y., Park, H.J., Hong, J.Y., Lee, H.J., and Lee, S.K. (2016). Down-regulation of SerpinB2 is associated with gefitinib resistance in non-small cell lung cancer and enhances invadopodia-like structure protrusions. Sci. Rep. 6, 32258.

22. Bach, D.-H., Park, H.J., and Lee, S.K. (2017). The dual role of bone morphogenetic proteins in cancer. Mol. Ther. Oncolytics 8, 1–13.

23. Qu, L., Ding, J., Chen, C., Wu, Z.J., Liu, B., Gao, Y., Chen, W., Liu, F., Sun, W., Li, X.F., et al. (2016). Exosome-transmitted lncARSR promotes sunitinib resistance in renal cancer by acting as a competing endogenous RNA. Cancer Cell 29, 653–668.

24. Luo, W., Huang, B., Li, Z., Li, H., Sun, L., Zhang, Q., Qiu, X., and Wang, E. (2013). MicroRNA-449a is downregulated in non-small cell lung cancer and inhibits migration and invasion by targeting c-Met. PLoS ONE 8, e64759.

25. Yamasaki, F., Johansen, M.J., Zhang, D., Krishnamurthy, S., Felix, E., Bartholomeusz, C., Aguilar, R.J., Kurisu, K., Mills, G.B., Hortobagyi, G.N., and Ueno, N.T. (2007). Acquired resistance to erlotinib in A-431 epidermoid cancer cells requires down-regulation of MMAC1/PTEN and up-regulation of phosphorylated Akt. Cancer Res. 67, 5779–5788.

26. Sos, M.L., Koker, M., Weir, B.A., Heynck, S., Rabinovsky, R., Zander, T., Seeger, J.M., Weiss, J., Fischer, F., Frommolt, P., et al. (2009). PTEN loss contributes to erlotinib resistance in EGFR-mutant lung cancer by activation of Akt and EGFR. Cancer Res. 69, 3256–3261.

27. Kokubo, Y., Gemma, A., Noro, R., Seike, M., Kataoka, K., Matsuda, K., Okano, T., Minegishi, Y., Yoshimura, A., Shibuya, M., and Kudoh, S. (2005). Reduction of PTEN protein and loss of epidermal growth factor receptor gene mutation in lung cancer with natural resistance to gefitinib (IRESSA). Br. J. Cancer 92, 1711–1719.

28. Yamamoto, C., Basaki, Y., Kawahara, A., Nakashima, K., Kage, M., Izumi, H., Kohno, K., Uramoto, H., Yasumoto, K., Kuwano, M., and Ono, M. (2010). Loss of PTEN expression by blocking nuclear translocation of EGR1 in gefitinib-resistant lung cancer cells harboring epidermal growth factor receptor-activating mutations. Cancer Res. 70, 8715–8725.

29. McCubrey, J.A., Steelman, L.S., Kempf, C.R., Chappell, W.H., Abrams, S.L., Stivala, F., Malaponte, G., Nicoletti, F., Libra, M., Bäsecke, J., et al. (2011). Therapeutic resistance resulting from mutations in Raf/MEK/ERK and PI3K/PTEN/Akt/mTOR signaling pathways. J. Cell. Physiol. 226, 2762–2781.

30. Maeda, M., Murakami, Y., Watari, K., Kuwano, M., Izumi, H., and Ono, M. (2015). CpG hypermethylation contributes to decreased expression of PTEN during acquired resistance to gefitinib in human lung cancer cell lines. Lung Cancer 87, 265–271.

31. Mao, M., Tian, F., Mariadason, J.M., Tsao, C.C., Lemos, R., Jr., Dayyani, F., Gopal, Y.N., Jiang, Z.Q., Wistuba, I.I., Tang, X.M., et al. (2013). Resistance to BRAF inhibition in BRAF-mutant colon cancer can be overcome with PI3K inhibition or demethylating agents. Clin. Cancer Res. 19, 657–667.

32. Hino, R., Uozaki, H., Murakami, N., Ushiku, T., Shinozaki, A., Ishikawa, S., Morikawa, T., Nakaya, T., Sakatani, T., Takada, K., and Fukayama, M. (2009). Activation of DNA methyltransferase 1 by EBV latent membrane protein 2A leads to promoter hypermethylation of PTEN gene in gastric carcinoma. Cancer Res. 69, 2766–2774.

33. Tazzari, P.L., Cappellini, A., Ricci, F., Evangelisti, C., Papa, V., Grafone, T., Martinelli, G., Conte, R., Cocco, L., McCubrey, J.A., and Martelli, A.M. (2007). Multidrug resistance-associated protein 1 expression is under the control of the phosphoinositide 3 kinase/Akt signal transduction network in human acute myelogenous leukemia blasts. Leukemia 21, 427–438.

34. Tazzari, P.L., Tabellini, G., Ricci, F., Papa, V., Bortul, R., Chiarini, F., Evangelisti, C., Martinelli, G., Bontadini, A., Cocco, L., et al. (2008). Synergistic proapoptotic activity of recombinant TRAIL plus the Akt inhibitor Perifosine in acute myelogenous leukemia cells. Cancer Res. 68, 9394–9403.

35. Chiarini, F., Del Sole, M., Mongiorgi, S., Gaboardi, G.C., Cappellini, A., Mantovani, I., Follo, M.Y., McCubrey, J.A., and Martelli, A.M. (2008). The novel Akt inhibitor, perifosine, induces caspase-dependent apoptosis and downregulates P-glycoprotein expression in multidrug-resistant human T-acute leukemia cells by a JNK-dependent mechanism. Leukemia 22, 1106–1116.

36. Bach, D.H., Kim, S.H., Hong, J.Y., Park, H.J., Oh, D.C., and Lee, S.K. (2015). Salternamide A suppresses hypoxia-induced accumulation of HIF-1α and induces apoptosis in human colorectal cancer cells. Mar. Drugs 13, 6962–6976.

37. Um, S., Bach, D.-H., Shin, B., Ahn, C.-H., Kim, S.-H., Bang, H.-S., Oh, K.B., Lee, S.K., Shin, J., and Oh, D.C. (2016). Naphthoquinone-oxindole alkaloids, coprisidins A and B, from a gut-associated bacterium in the dung beetle, Copris tripartitus. Org. Lett. 18, 5792–5795.

38. Peng, Y., Sartini, D., Pozzi, V., Wilk, D., Emanuelli, M., and Yee, V.C. (2011). Structural basis of substrate recognition in human nicotinamide N-methyltransferase. Biochemistry 50, 7800–7808.

39. Santarelli, L., Strafella, E., Staffolani, S., Amati, M., Emanuelli, M., Sartini, D., Pozzi, V., Carbonari, D., Bracci, M., Pignotti, E., et al. (2011). Association of MiR-126 with soluble mesothelin-related peptides, a marker for malignant mesothelioma. PLoS ONE 6, e18232.

40. Zhang, Y.W., Staal, B., Essenburg, C., Su, Y., Kang, L., West, R., Kaufman, D., Dekoning, T., Eagleson, B., Buchanan, S.G., and Vande Woude, G.F. (2010). MET kinase inhibitor SGX523 synergizes with epidermal growth factor receptor inhibitor erlotinib in a hepatocyte growth factor-dependent fashion to suppress carcinoma growth. Cancer Res. 70, 6880–6890.

41. Stambolic, V., Suzuki, A., de la Pompa, J.L., Brothers, G.M., Mirtsos, C., Sasaki, T., Ruland, J., Penninger, J.M., Siderovski, D.P., and Mak, T.W. (1998). Negative regulation of PKB/Akt-dependent cell survival by the tumor suppressor PTEN. Cell 95, 29–39.

42. Fry, M.J. (2001). Phosphoinositide 3-kinase signalling in breast cancer: how big a role might it play? Breast Cancer Res. 3, 304–312.

43. Bach, D.-H., Liu, J.-Y., Kim, W.K., Hong, J.-Y., Park, S.H., Kim, D., Qin, S.N., Luu, T.T., Park, H.J., Xu, Y.N., and Lee, S.K. (2017). Synthesis and biological activity of new phthalimides as potential anti-inflammatory agents. Bioorg. Med. Chem. 25, 3396–3405.

44. Chou, T.C. (2006). Theoretical basis, experimental design, and computerized simulation of synergism and antagonism in drug combination studies. Pharmacol. Rev. 58, 621–681.